Optical Materials 31 (2009) 931–935

Contents lists available at ScienceDirect

Optical Materials

journal homepage: www.elsevier.com/locate/optmat

Nonlinear optical properties of composite films consisting of multi-armed CdS nanorods and ZnO

Tingyin Ning, Peng Gao, Wenlong Wang, Heng Lu, Wangyang Fu, Yueliang Zhou *, Dongxiang Zhang, Xuedong Bai, Enge Wang, Guozhen Yang

Beijing National Laboratory for Condensed Matter Physics, Institute of Physics, Chinese Academy of Sciences, Beijing 100190, People's Republic of China

ARTICLE INFO

Article history:
Received 17 April 2008
Received in revised form 22 October 2008
Accepted 22 October 2008
Available online 6 December 2008

PACS:
42.65.Hw
42.70.Nq
78.66.Hf
78.67.Pt

Keywords:
CdS
Multi-armed nanorods
Nonlinear optics
Z-scan

ABSTRACT

The multilayer composite films consisting of multi-armed CdS nanorods and ZnO were fabricated by spin coating and pulsed laser deposition on fused quartz substrates. The nonlinear optical properties such as nonlinear refraction and absorption were determined using closed- and open-aperture Z-scan method with 532 nm picosecond and 800 nm femtosecond laser pulses, respectively. The nonlinear optical response time was studied by a time resolved Kerr-gate technique at 800 nm, showing an instantaneous process. The large optical nonlinearity with ultrafast response of the composite films indicated their potential applications for future nonlinear optical devices.

1. Introduction

Nonlinear optical materials with large third-order nonlinear optical susceptibility $\chi^{(3)}$ and small relaxation time of photocarries have been widely studied because of the potential applications in optical bistability, optical computing and optical phase-conjugation [1–3]. Nanometer-sized semiconductor materials have been intensively investigated since they exhibit large optical nonlinearity and fast response time due to their novel electric structures originated from quantum-confine effect and interfacial effect [4–11]. Compared with nanoparticles, one-dimensional (1D) semiconductor nanorods or nanowires are drawing more attention due to their particular structures [12–16]. Especially, the more complicated 1D nanostructure such as multi-armed nanorods, which have two or more limbs connected at a central core, were synthesized by many groups recently and would provide more opportunities to the applied field [17–20]. Greeham and his co-workers reported that the blends of branched CdSe nanorods with conjugated polymers could improve the efficiency of hybrid photovoltaic devices [21]. Cui et al. have studied a new single-electron transistor operation scheme enabled by multi-armed CdTe nanorods indicating a very useful structure for electric devices [22]. The linear optical properties, such as optical absorption, photoluminescence spectra, Raman scattering of the multi-armed nanorods have also been widely studied [19,23]. However, the nonlinear optical properties of the multi-armed nanorods have not been investigated as far as we know.

In this paper, we report nonlinear optical properties of the composite films, which were formed by combining multi-armed CdS nanorods with the other semiconductor material ZnO using spin coating and pulsed laser deposition. The large optical nonlinearities of the composite films were obtained.

2. Experimental details

2.1. Composite films fabrication

The CdS nanorods with multi-arms were synthesized via aqueous chemical growth route at room temperature. The procedure was described in detail elsewhere [20]. The product was obtained by centrifugation and washed with deionized water and ethanol. The purified CdS nanorods are well dispersed in ethanol or in

* Corresponding author. Tel.: +86 10 82648108; fax: +86 10 82649356.
E-mail address: ylzhou@aphy.iphy.ac.cn (Y. Zhou).

0925-3467/$ - see front matter © 2008 Elsevier B.V. All rights reserved.
doi:10.1016/j.optmat.2008.10.041

aqueous solutions. The final CdS nanocrystals are with a mixture of one-, two-, three-, and four-armed rods. The lengths of the arms are not very uniform, while their diameters have a relatively narrow size distribution (about 5 nm). The concentration of CdS nanorods used in the experiments was about 0.5 mg/ml in ethanol. All the films combining these CdS nanorods with ZnO were fabricated onto fused quartz substrates of 0.5 mm in thickness with both sides polished. Firstly, ZnO layer with thickness about $60 \sim 70$ nm was deposited on the substrate in pure O_2 atmosphere (10 Pa) at room temperature using pulsed laser deposition (PLD) technique. Then, 150 μl of ethanol containing CdS nanorods were dispersed on the ZnO layer by spin coating with the speed of 3000 rpm. The quantity of CdS nanorods was controlled by adjusting the quantity of the droplet. The samples were fabricated by depositing ZnO film layer and CdS nanorods layer alternatively. The sample with five layers was selected to be discussed here. The thickness of the sample was about 210 nm determined by scanning electron microscopy (SEM).

2.2. Physical measurements

The nanostructure of CdS nanorods was investigated by transmission electron microcopy (TEM). The surface morphology of the composite films was characterized by atomic force microscopy (AFM). Linear optical absorption measurements of the samples were performed in the air from 330 nm to 800 nm using a SpectraPro-500i spectrophotometer (Acton Research Corporation) at room temperature. The absorption spectra were corrected automatically considering the absorbance of fused quartz substrates. The third-order optical nonlinearities of the composite films were characterized using the single beam Z-scan technique, which could separate the contributions of refractive and absorptive nonlinearities in the samples. A typical Z-scan experimental setup we used was shown in Fig. 1. In the experiment, a mode-locked Nd:YAG laser with frequency doubled at a wavelength of 532 nm and a pulsed duration of 25 ps was used as the light source in the picosecond regime. The repetition rate was set to 1 Hz. In the femtosecond time regime, femtosecond laser pulses were obtained from a conventional chirped pulse amplification system comprising of a Ti:sapphire oscillator (Tsunami, Spectra-Physic Inc.) that delivered ~120 fs, 82 MHz at 800 nm and a regenerative Ti:sapphire amplifier (TSA-10, Spectra-Physic Inc.), from which we obtained 10 Hz amplified pulses of ~200 fs, with output energy of ~5 mJ. The laser energy was adjusted using neutral optical attenuators during the Z-scan experiment. The laser beam was focused onto the sample by a 150 mm focal length lens. The beam waists were measured to be about 25 μm for ps excitation and 34 μm for fs excitation. The peak intensities used in experiments were in the 6–14 GW/cm^2 and 150–300 GW/cm^2 ranges for ps and fs pulse excitation, respectively. The on-axis transmitted beam energy, the reference beam energy, and the ratios of them were measured using an energy ratiometer (EPM 2000, Coherent Inc.).

To determine the third-order nonlinear optical response of the composite film, a standard femtosecond optical Kerr-effect (OKE)

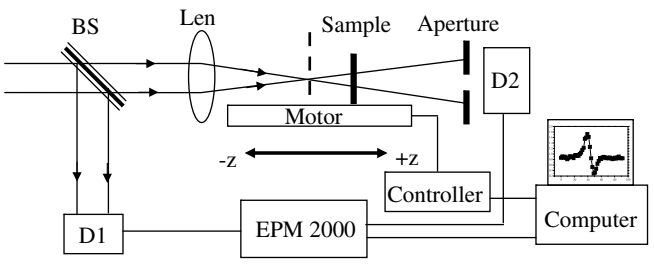

Fig. 1. Experimental setup for Z-scan.

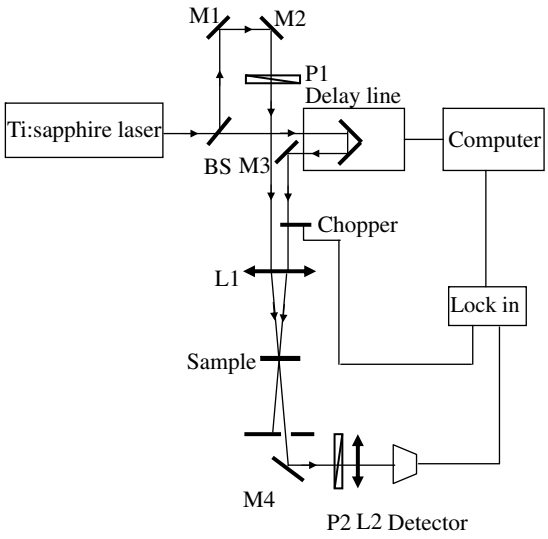

Fig. 2. Experimental setup for femtosecond OKE measurement.

experiment was performed [24,25]. The experimental apparatus was shown in Fig. 2. The Ti:sapphire oscillator (800 nm, 82 MHz, ~120 fs), which was described above, was used as the light source. The pulse train was split into an intense pump and a weak probe beam, which had an average power of 30 mW and 2.8 mW, respectively. The pump beam was modulated at a frequency of about 1 kHz by a chopper after passing through a variable line controlled by a computer. The polarization of the probe beam was rotated 45° with respect to the pump beam by a polarizer. The two beams were focused by a lens to overlap in the sample. The transmitted probe beam passed through an analyzer with the polarization perpendicular to the original polarizer. The generated optical Kerr signal was detected by a photodiode detector connected with a lock-in amplifier (SR830, Stanford, USA). The data were collected using a computer program. The zero delay time point was determined using a 1 mm-thick BBO crystal.

3. Results and discussion

3.1. Surface morphology of the sample

The TEM images of CdS nanorods have been shown elsewhere and the multi-armed structures can be clearly seen [20]. Fig. 3 shows 2D and 3D AFM images 1×1 μm^2 area of surface morphology of the top layer ZnO film. The images show the regular fluctuation profile of ZnO film due to the dispersed CdS multi-armed nanorods in an almost order orientation. The maximum height fluctuation is about 4.7 nm and the root-mean-square surface roughness is about 1.1 nm, suggesting good smoothness of the film.

3.2. Linear optical absorption

The linear optical absorption spectra are shown in Fig. 4. As a reference, the optical absorption spectrum of undoped ZnO was also recorded in Fig. 4a. The absorption peak near 365 nm arose from the excition absorption of ZnO nanocrystallites. The inset shows the linear optical absorption of pure CdS nanorods dispersed in ethanol solution. The absorption band around 450 nm indicates the blue-shift compared to the bulk band absorption of 512 nm due to the quantum-confine effect. The absorption peak of CdS nanorods is not shown obviously in the spectrum of composite film in Fig. 4b. The reason may be that the amount of the CdS nanorods is too small. The linear optical absorption coefficient α is about 8.4×10^3 cm^{-1} at 532 nm and tends to zero at 800 nm.

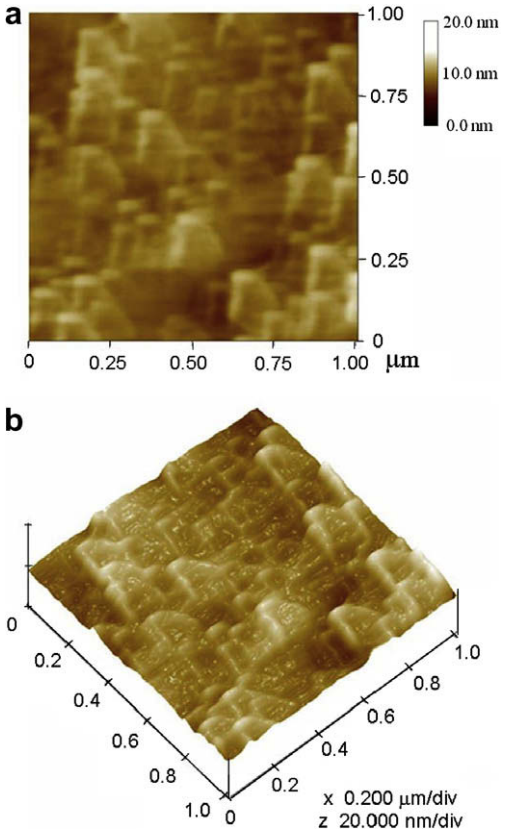

Fig. 3. (a) 2D and (b) 3D AFM images of composite film.

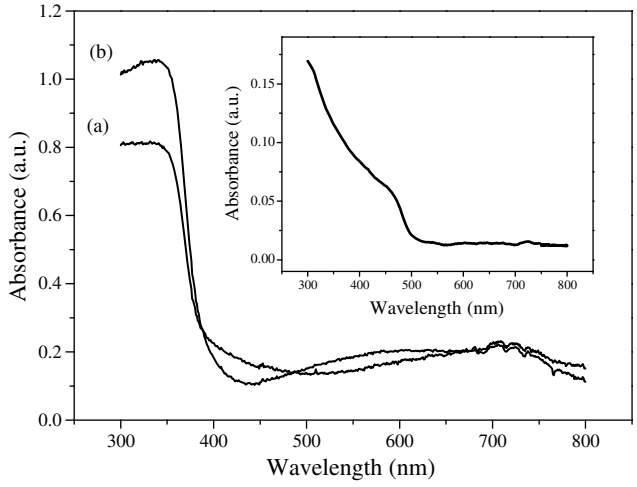

Fig. 4. The linear optical absorption properties of (a) pure ZnO film and (b) ZnO/CdS composite film. The inset shows the optical spectrum of pure CdS nanorods dispersed in ethanol solution.

3.3. Nonlinear optical properties with 532 nm, 25 ps pulses Z-scan studies

The typical Z-scan curve of the sample for an open-aperture (OA) was shown in Fig. 5a, normalized transmittance as a function of the sample position Z at peak irradiance $I_0 = 6.0\ \mathrm{GW/cm^2}$. The filled squares indicate the measured data, with each point corresponding to the average value of 10 pulses. The corresponding solid lines represent their theoretical fittings using the equation as follows [26],

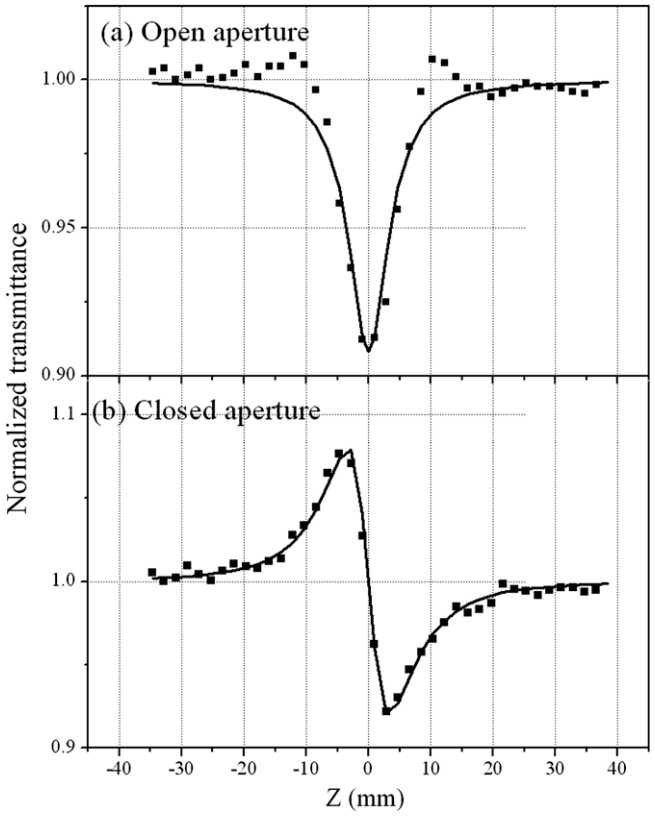

Fig. 5. The Z-scan data of sample with (a) an open and (b) a closed-aperture measured at 532 nm with pulse duration 25 ps. The solid lines indicate the theoretical fit.

$$T(z, S=1) = \sum_{m=0}^{\infty} \frac{[-q_0(z)]^m}{(m+1)^{3/2}} \quad \text{for } |q_0| < 1 \tag{1}$$

where $q_0(z) = \beta I_0 L_{eff}/(1 + z^2/z_0^2)$, I_0 is the laser peak intensity, $L_{eff} = [1 - \exp(-\alpha L)]/\alpha$ is the effective thickness of the films (L is the sample thickness) and z_0 is the diffraction length of the beam. The obtained nonlinear absorption coefficient β and imaginary part of $\chi^{(3)}$, $\mathrm{Im}\chi^{(3)}$, can be calculated to be 2.0×10^{-8} m/W and 8.6×10^{-10} esu, respectively.

The close-aperture (CA) curve was obtained after division of CA data with the OA data to eliminate the contribution of nonlinear absorption and is shown in Fig 5b. The peak-valley configuration indicates the negative nonlinearity of the sample, which is accord of the results calculated by Sheik–Bahae and co-workers using two-band, effective-mass model [4]. The plot of the normalized transmittance $T(z)$ is fitted by the equation,

$$T(z) = 1 - \frac{4z/z_0}{(z^2/z_0^2 + 9)(z^2/z_0^2 + 1)}\Delta\Phi_0 \tag{2}$$

and

$$\Delta T_{p-v} = 0.406(1 - S)^{0.25}|\Delta\Phi_0| \quad \text{for } |\Delta\Phi_0| \leqslant \pi \tag{3}$$

where $\Delta\Phi_0$ is the on-axis phase shift at the focus, ΔT_{p-v} is the difference between the normalized peak and valley transmittance. The linear transmittance of the far-field aperture, S, defined as the ratio of the pulse energy passing through the aperture to the total energy. The measured values of nonlinear refractive index n_2 and real part of $\chi^{(3)}$, $\mathrm{Re}\chi^{(3)}$,were $-2.9 \times 10^{-15}\ \mathrm{m^2/W}$ and -2.9×10^{-9} esu, respectively. The absolute value of $\chi^{(3)}$ and the figure of merit ($\chi^{(3)}/\alpha$) were calculated to be about 3.0×10^{-9} esu and 3.6×10^{-13} esu cm, respectively. The value of third-order nonlinear optical susceptibility of the composite film was about one to two orders

of magnitude larger than that of pure ZnO film and some composite materials containing CdS nanoparticles [8,9,27], and was comparable with that of the transition-metal oxide films with large optical nonlinearities, such as Cr_2O_3, Mn_3O_4, Fe_2O_3, Co_2O_3, CuO and so on [28].

The measurements of intensity dependent behaviors of β and n_2 were carried out at the different on-axis peak intensity I_0, varied from 6 to 14 GW/cm^2. Fig. 6 shows the relations of normalized transmittance T and ΔT_{p-v} as a function of incident intensity. The linear relation with no significant deviation from the intensity dependence indicated the third-order nonlinearity. The relative uncertainty was about 20% in our experiment, which is typical value of Z-scan measurement.

3.5. Nonlinear optical properties with 800 nm, femtosecond pulses Z-scan and OKE studies

Fig. 7 shows the representative OA and CA curves of Z-scan measurements at a wavelength of 800 nm with laser duration of 200 fs. The energy of a single laser pulse was about 2 μJ, corresponding to an input irradiance of about 275 GW/cm^2. The experimental data were fitted using Eqs. (1) and (2). The nonlinear optical absorption coefficient β and imaginary part of $\chi^{(3)}$, Im$\chi^{(3)}$, can be calculated to be 7.1×10^{-10} m/W and 4.6×10^{-11} esu. And

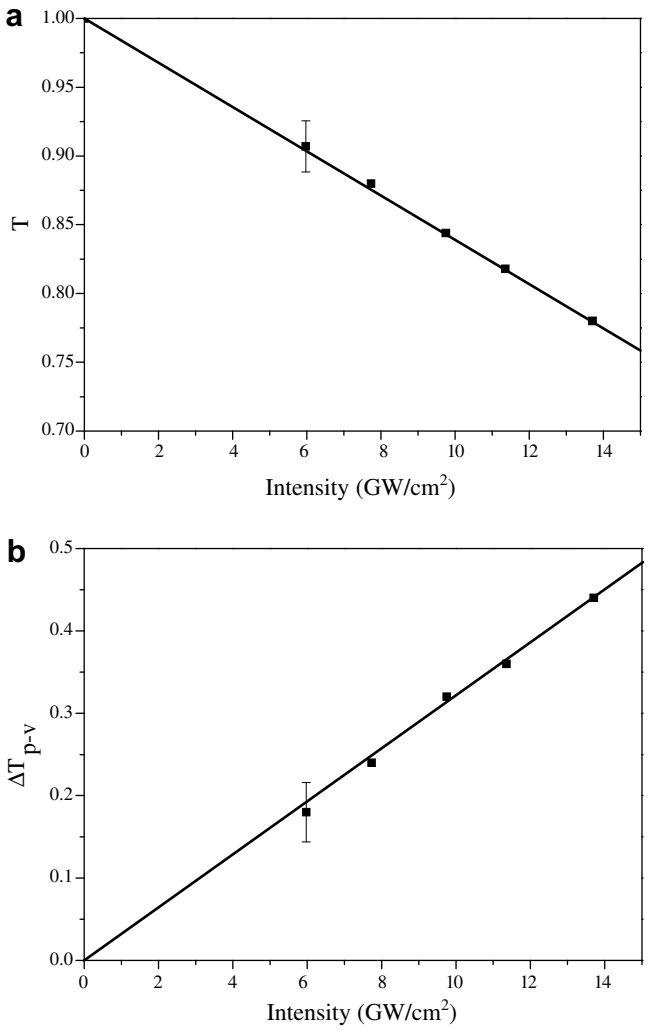

Fig. 6. (a) The normalized transmittance T when OA and (b) ΔT_{p-v}, the difference between the normalized peak and valley transmittance when CA, vs peak intensity I_0 for composite material. The linear relations indicate a third-order process.

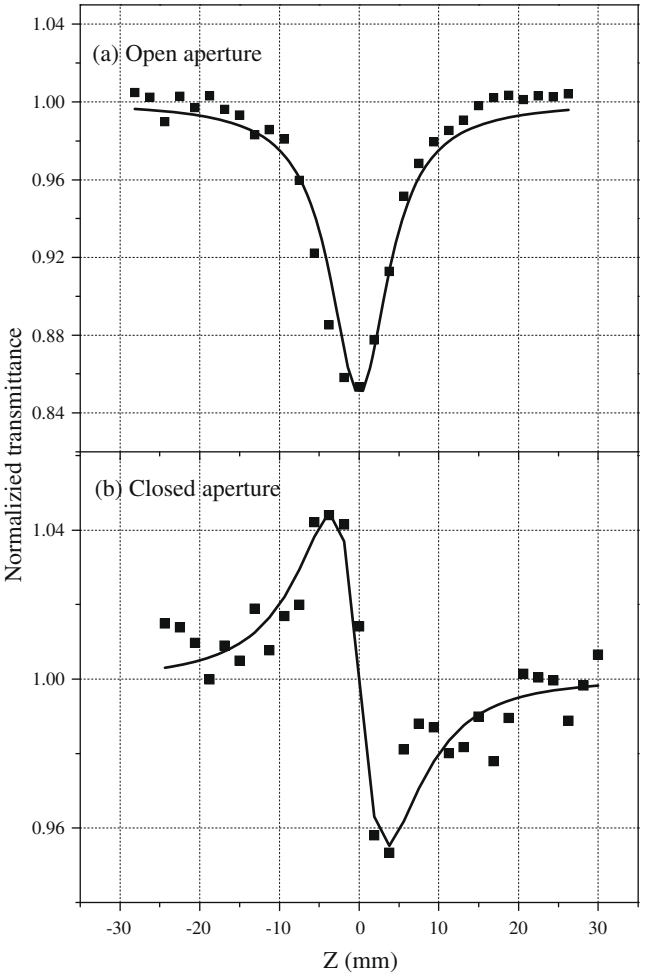

Fig. 7. The Z-scan data of sample with (a) an open and (b) a closed-aperture measured at 800 nm with pulse duration 200 fs. The solid lines indicate the theoretical fit.

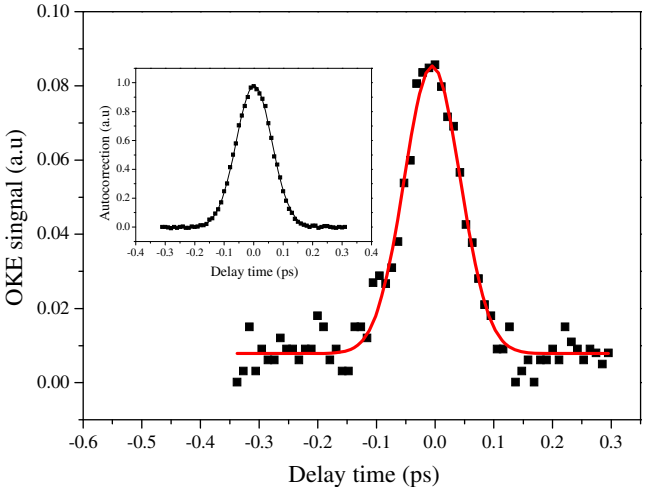

Fig. 8. Time resolved optical Kerr-effect signal of CdS/ZnO composite film measured at 800 nm.

the measured values of nonlinear refractive index n_2 and real part of $\chi^{(3)}$, Re$\chi^{(3)}$, were estimated to be -4.7×10^{-17} m^2/W and -4.8×10^{-11} esu, respectively. The absolute value of $\chi^{(3)}$ were calculated to be about 6.6×10^{-11} esu accordingly, which was about

one order of magnitude larger than bulk CdS material [29], and was comparable with the values of CdS nanoclusters embedded in the organic films [30]. The measurements were performed at different laser irradiances. The linear relation of ΔT_{p-v} vs I_0 indicated the third-order nonlinearity.

The nonlinear optical response of the composite film was determined using OKE technique. The measured autocorrelation curve was shown in the left corner of Fig. 8. The typical ultrafast OKE signal obtained in CdS nanorods/ZnO composite film was shown in Fig. 8. The symmetrical signal curve corresponds nearly to the laser pulse profile, implying that third-order nonlinear linear optical response of the sample was instantaneous. This ultrafast response was mainly attributed to nonresonant electronic nonlinearities.

4. Conclusions

The multilayer composite films consisting of CdS multi-armed nanorods and ZnO were fabricated layer by layer using spin coating and pulse laser deposition technique on fused quartz substrates. The third-order nonlinear optical properties of the composite films were determined by Z-scan method at a wavelength of 532 nm with pulse duration of 25 ps and a wavelength of 800 nm with pulse duration of 200 fs, respectively. The third-order nonlinear optical absorption coefficient β and nonlinear refractive index n_2, were obtained, respectively. The ultrafast nonlinear optical response was determined using OKE technique at 800 nm. The large and ultrafast response optical nonlinearity of the composite films indicated their potential applications for future nonlinear optical devices.

Acknowledgement

The authors are grateful for the financial support of National Natural Science Foundation of China (Grant No. 50532090).

References

[1] D. Ricard, P. Roussignol, C. Flytzanis, Opt. Lett. 10 (1985) 511.
[2] D. Cotter, R.J. Manning, K.J. Blow, A.D. Ellis, A.E. Kelly, D. Nesset, I.D. Phillips, A.J. Poustie, D.C. Rogers, Science 286 (1999) 1523.
[3] A. Hache, M. Bourgeois, Appl. Phys. Lett. 77 (2000) 4089.
[4] M. Sheik-Bahae, D.J. Hagan, E.W. Van Stryland, Phys. Rev. Lett. 65 (1990) 96.
[5] D. Cotter, M.G. Burt, R.J. Manning, Phys. Rev. Lett. 68 (1992) 1200.
[6] Y. Wang, Acc. Chem. Res. 24 (1991) 133.
[7] Y.B. Han, J.B. Han, S. Ding, D.J. Chen, Q.Q. Wang, Opt. Exp. 13 (2005) 9211.
[8] R.E. Schwerzel, K.B. Spahr, J.P. Kurmer, V.E. Wood, J.A. Jenkins, J. Phys. Chem. A 102 (1998) 5622.
[9] N. Sugimoto, A. Koiwai, S. Hyodo, T. Hioki, S. Noda, Appl. Phys. Lett. 66 (1995) 923.
[10] Y. Gao, A. Tonizzo, A. Walser, M. Potasek, R. Dorsinville, Appl. Phys. Lett. 92 (2008) 033106.
[11] L. Irimpan, V.P.N. Nampoori, P. Radhakrishnan, B. Krishnan, A. Deepthy, J. Appl. Phys. 103 (2008) 033105.
[12] J. Hu, L.-S. Li, W. Yang, L. Manna, L.-W. Wang, A.P. Alivisatos, Science 292 (2001) 2060.
[13] Y. Cui, C.M. Lieber, Science 291 (2001) 851.
[14] X. Peng, L. Manna, W. Yang, J. Wickham, E. Scher, A. Kadavanich, A.P. Alivisatos, Nature 404 (2000) 59.
[15] M.B. Mohamed, C. Burda, M.A. El-Sayed, Nano Lett. 1 (2001) 589.
[16] A. Shabaev, Al.L. Efros, Nano Lett. 4 (2004) 1821.
[17] L. Manna, E.C. Scher, A.P. Alivisatos, J. Am. Chem. Soc. 122 (2001) 12700.
[18] Y.W. Jun, S.M. Lee, N.J. Kang, J. Cheon, J. Am. Chem. Soc. 123 (2001) 5150.
[19] F. Gao, Q. Li, S. Xie, D. Zhao, Adv. Mater. 21 (2002) 1537.
[20] W. Wang, F. Bai, Chem. Phys. Chem. 4 (2003) 761.
[21] B. Sun, E. Marx, N.C. Greenham, Nano Lett. 3 (2003) 961.
[22] Y. Cui, U. Banin, M.T. Bjork, A.P. Alivisatos, Nano Lett. 5 (2005) 1519.
[23] L. Manna, D.J. Milliron, A. Meisel, E.C. Scher, A.P. Alivisatos, Nature 2 (2003) 382.
[24] P. Foggi, R. Righini, R. Torre, V.F. Kamalov, Chem. Phys. Lett. 193 (1992) 23.
[25] Q.H. Gong, J.L. Li, T.Q. Zhang, H. Yang, Chin. Phys. Lett. 15 (1998) 30.
[26] M. Sheik-Bahae, A.A. Said, T.H. Wei, D.J. Hagan, W. Van Stryland, IEEE J. Quant. Electron. 26 (1990) 760.
[27] X.J. Zhang, W. Ji, S.H. Tang, J. Opt. Soc. Am. B 14 (1997) 1951.
[28] M. Ando, K. Kadono, M. Haruta, T. Sakaguchi, M. Miya, Nature 374 (1995) 625.
[29] Noriaki Sugimoto, Akihiko Koiwai, Shi-aki Hyodo, Tatsumi Hioki, Shoji Noda, Appl. Phys. Lett. 66 (2005) 923.
[30] J. He, W. Ji, G.H. Ma, S.H. Tang, E.S.W. Kong, S.Y. Chow, X.H. Zhang, Z.L. Hua, J.L. Shi, J. Phys. Chem. B 109 (2005) 4373.